Recent Progress in Wide-Field Imaging Interferometry

S. A. Rinehart[1a], D. T. Leisawitz[a], M. R. Bolcar[a], K. M. Chaprnka[a], R. G. Lyon[a], S. F. Maher[b], N. Memarsadeghi[a], E. J. Sinukoff[c], E. Teichman[d]
[a]NASA Goddard Space Flight Center, Greenbelt MD 20771
[b]Science Systems and Applications, Inc., Greenbelt MD 20771
[c]McMaster University, Hamilton, ON L8S4L8
[d]University of Maryland, College Park, MD 20742

ABSTRACT

The Wide-Field Imaging Interferometry Testbed (WIIT) at NASA's Goddard Space Flight Center and a computational model of the testbed were developed to demonstrate and learn the practical limitations of techniques for wide-field spatial-spectral ("double Fourier") interferometry. WIIT is an automated and remotely operated system, and it is now producing substantial amounts of high-quality data from its state-of-the-art operating environment, Goddard's Advanced Interferometry and Metrology Lab. In this paper, we discuss the characterization and operation of the testbed and present recently acquired data. We also give a short description of the computational model and its applications. Finally, we outline future research directions. A companion paper within this conference discusses the development of new wide-field double Fourier data analysis algorithms.

Keywords: Interferometry, double-Fourier, testbed, wide-field imaging

1. INTRODUCTION

NASA's Wide-Field Imaging Interferometry project is designed to demonstrate the practicality of obtaining high angular resolution integral field spectroscopy over a wide field of view at long wavelengths, where a single aperture telescope would have to be impractically large to provide comparable resolution. This technique will have significant value for future space-based interferometric missions, opening new regimes in measurement space to address a wide range of astronomical questions. As previously reported (Rinehart, et al. 2006), we have used the Wide-field Imaging Interferometry Testbed (WIIT) to demonstrate the fundamental techniques required for wide-field interferometric imaging. With continued research we expect to bring this technique/technology to TRL 6 by 2012.

1.1 Motivation for Wide-Field Imaging Interferometry

Infrared observations from missions such as the Infrared Space Observatory (ISO), *Spitzer*, and *Herschel* have demonstrated the importance of these long wavelengths for understanding a wide array of astronomical sources. However, these observations also provide hints at much more information that lurks at smaller angular scales. To achieve Hubble-class angular resolution in the far-infrared would require a single aperture telescope of order 1 km in diameter. Alternatively, interferometry can allow us to obtain high angular resolution with ample sensitivity at these long wavelengths. With a future space-based interferometer operating in the FIR and submillimeter, we will be able to observe dust structures within circumstellar disks (e.g. debris disks), resolve individual sources in deep sky images (e.g. the Hubble Deep Field) by eliminating source confusion, and learn how molecular material is distributed around nearby stars. Such a mission will build directly on the successes of past (IRAS, ISO), present (*Spitzer, Herschel)*, and upcoming (SPICA) far-infrared missions, and will pave the way for interferometers operating at shorter wavelengths designed to image exoplanets and to search for life in the universe. For all of these goals, the ability to obtain high angular resolution over relatively large fields of view will be critical.

[1] Contact S. Rinehart at Stephen.A.Rinehart@nasa.gov , ph: 301-286-4591

Optical and Infrared Interferometry II, edited by William C. Danchi, Françoise Delplancke, Jayadev K. Rajagopal,
Proc. of SPIE Vol. 7734, 77342D · © 2010 SPIE · CCC code: 0277-786X/10/$18 · doi: 10.1117/12.857108

Downloaded From: http://spiedigitallibrary.org/ on 05/24/2017 Terms of Use: http://spiedigitallibrary.org/ss/termsofuse.aspx

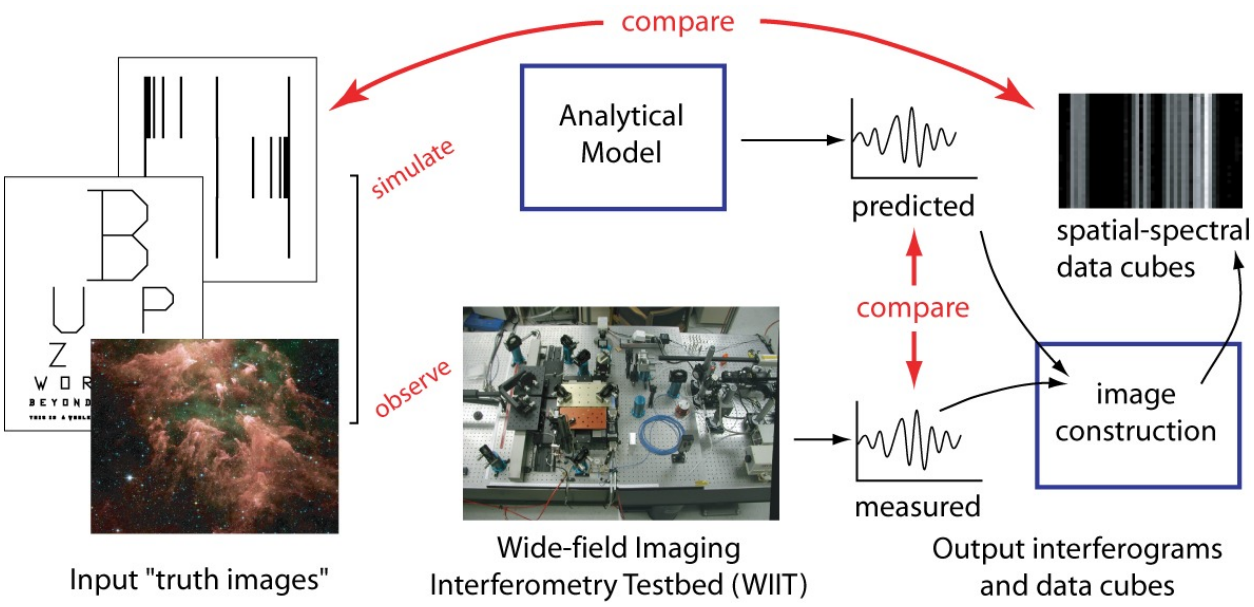

Figure 1: Our experimental approach makes use of both data acquired with the WIIT and with a high-fidelity computer model of the testbed. By comparing the measured fringe pattern to that predicted by the model, we are able to understand the limitations and capabilities of the testbed. The testbed and the model both yield interferograms from which spatial-spectral data cubes are synthesized and compared with direct measurements of the scenes observed interferometrically, or modeled computationally.

1.2 A Brief History of WIIT

WIIT was originally conceived as a tool for demonstrating the practicality of wide-field spatial-spectral interferometry for future space-based as application on the Submillimeter Probe of the Evolution of Cosmic Structure (SPECS; Rinehart, 2006; Harwit, et al. 2008). By operating in a "double-Fourier" mode of operation (Mariotti & Ridgeway 1988), such an interferometer can simultaneously obtain both spatial and spectral data. However, traditional Michelson interferometers use a single detector element, and are limited to a field-of-view corresponding to the diffraction limit of the individual collector telescopes (~λ/2D). By replacing the single detector element with a detector array, however, one can obtain spectral and spatial information over a wide field-of-view. In addition to demonstrating this capability, WIIT was designed to explore the effects of systematics on data quality (Feinberg, et al. 2000). WIIT provides real-world data that can be used to test and refine algorithms and techniques for wide-field, double-Fourier interferometry. This will be valuable for future missions such as SPECS, the Space Infrared Interferometric Telescope (SPIRIT; Leisawitz et al. 2007; http://astrophysics.gsfc.nasa.gov/cosmology/spirit), and balloon experiments such as the Balloon Experimental Twin Telescope for Infrared Interferometry (BETTII; Rinehart 2010).

Previous papers have provided details on the development and capabilities of WIIT (e.g. Rinehart, et al. 2008; Leisawitz, et al. 2003). In this paper, we discuss recent developments and the plan for continued research with WIIT. Excluded from this discussion is the development of new algorithms for analyzing data produced using wide-field interferometric techniques; this is the subject of a companion paper presented at this meeting (Lyon, et al. 2010).

1.3 Experimental Approach

Our experimental approach was designed to demonstrate wide-field spatial-spectral interferometry and enable a thorough understanding of its practical limitations (Figure 1) by following a dual-path approach. The WIIT testbed, discussed in more detail below, allows us to generate data that directly tests the approach. By operating in the Advanced Interferometry and Metrology (AIM) Laboratory at Goddard, we ensure a high-quality, stable environment that allows us to produce high-quality data. Previously developed automation of the system allows us to collect large amounts of data while minimizing the need for interaction with the testbed itself. This helps prevent disturbance of the operating environment and helps maintain environmental stability. Using the algorithms being developed for wide-field imaging interferometry, we can reconstruct the source image from the testbed data.

Downloaded From: http://spiedigitallibrary.org/ on 05/24/2017 Terms of Use: http://spiedigitallibrary.org/ss/termsofuse.aspx

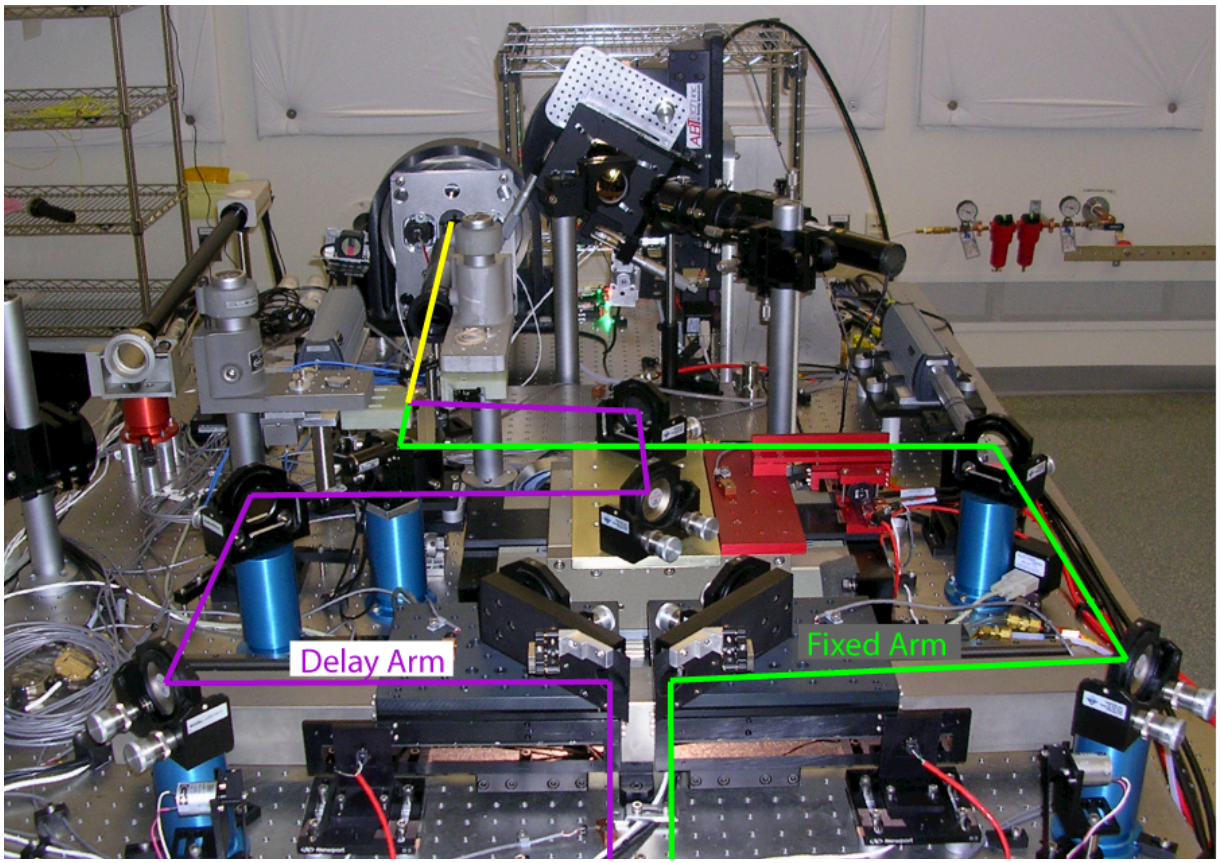

Figure 2: The Wide-Field Imaging Interferometry Testbed WIIT). The green line in the figure traces the optical path for the fixed arm of the interferometer, while the purple line traces the delay line path.

The second path of our approach uses a high-fidelity computational model of the hardware testbed, WIIT. We are using the model to produce simulated interferometric data sets of several types. First, a model of WIIT with no imperfections will yield "error-free data." These "data" can be compared directly with data from the testbed to understand and calibrate instrumental effects, such as visibility loss, and they can be used to synthesize spatial-spectral data cubes to test the synthesis algorithms. We verify that the model, with all error sources activated, produces simulated data consistent with the actual data from WIIT to within the uncertainty associated with counting fluctuations in the detection process. Second, we can add optical component imperfections and artificial detector shot noise to the model to understand the individual sources of error and visibility loss, such as low- and mid-spatial frequency mirror surface imperfections, and wavelength-dependent beamsplitter reflectivity. Our computational model can also be used to test the spatial noise distribution predicted by theory for an ideal interferometer (Prasad and Kulkarni 1989). Third, we will empirically determine how individual error sources propagate to the "constructed" data cubes by comparing the input "truth" and output "constructed" data cubes based on model interferometric data with a single error source activated at a time. A microscope equipped with a digital camera was used to record input "truth" images.

1.4 The Testbed

The testbed has been described in detail in previous papers, but for completeness we briefly describe it here. WIIT is a 1:150 scale model of SPIRIT, operating at optical wavelengths. A picture of WIIT in the AIM lab is shown in Figure 2; a solid-body model of the testbed is shown in Figure 3. Light from the test scene, located at the focus of the collimating mirror, is projected into the interferometer. The two collector mirrors feed the two arms of the interferometer. One of these arms consists solely of fixed flat mirrors (the "fixed" arm), while the other includes a pair of mirrors mounted on the delay line stage in a rooftop configuration (the "delay" arm). The delay line scans a range of optical path difference between the two arms of the interferometer. The beams from the two arms are recombined within the beamsplitter, and the output from one of the two output ports is focused onto a CCD camera. The source stage can be rotated, providing

Downloaded From: http://spiedigitallibrary.org/ on 05/24/2017 Terms of Use: http://spiedigitallibrary.org/ss/termsofuse.aspx

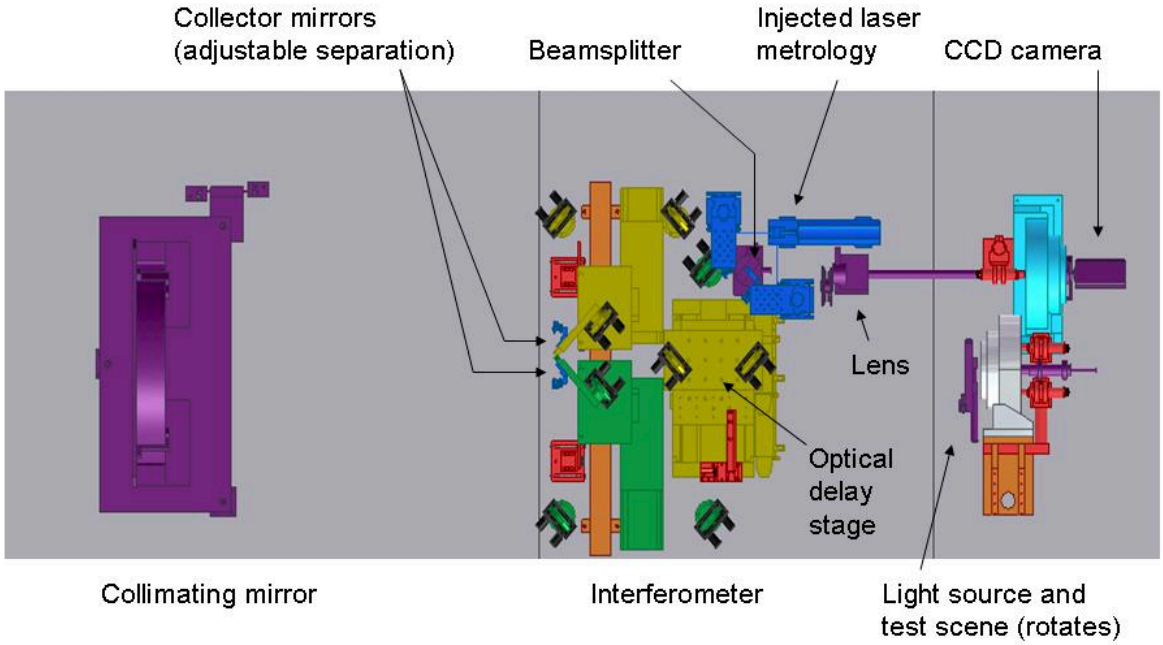

Figure 3: This top view of WIIT, generated from a 3-D solid model, shows all of the major elements of the testbed. (*u*-*v*) plane coverage is provided by two linear stages upon which the collector mirrors are mounted, and by two rotation stages upon which the source scene and the camera are mounted. The injected metrology system measures the actual optical pathlength of both arms of the interferometer in real time, providing important ancillary data for interpretation of the scientific data.

access to all possible baseline orientations. The collector mirrors can be moved along a straight rail to vary baseline length.

The novel aspect of WIIT is the use of a detector array (a CCD camera, in this case) instead of the single-pixel detector used in a traditional Michelson interferometer. Each pixel on the detector records light arriving from a different part of the sky (test scene). As the delay line is scanned, each pixel records an interferogram unique to the field angle corresponding to the pixel. By using observations at a wide range of *u*-*v* points, reconstructed images can be produced for each pixel; these images can then be mosaiced together, producing a wide field-of-view image with the full interferometric angular resolution. In reality, a more sophisticated algorithm is used to generate a spatial-spectral data cube covering the wide field of view. By providing a long delay line scan, we are further able to obtain spectral information for the observed sources; to obtain a resolution R requires an optical path delay scan range of $\delta = R\lambda$.

The interferometric fringes have different relative phases for the different detector pixels, due to the geometric optical delay inherent for sources off the axis of the interferometer. Therefore, to obtain data on the full fringe packet for each point within the full field-of-view, we require an optical delay stroke larger than the scan range required for spectroscopy.

2. DATA ACQUISITION

Previously, WIIT was used to demonstrate the fundamentals of wide-field imaging interferometery, by observing multiple bright sources dispersed in one dimension (Rinehart et al. 2006). By automating the testbed, we enabled a much higher data acquisition rate (Rinehart, et al. 2008). Over the past two years, we have been acquiring data for a wide variety of sources, covering a full range of baselines. With the fully automated system, we obtained data for a series of source images of "binary stars." Each source image in the series consists of two pinholes (both pinhole sources are of the same size and brightness, and have the same spectrum). In the first source image of the series, the two sources are closely spaced, such that they are barely resolved at even the longest baselines. The separation between the two

Downloaded From: http://spiedigitallibrary.org/ on 05/24/2017 Terms of Use: http://spiedigitallibrary.org/ss/termsofuse.aspx

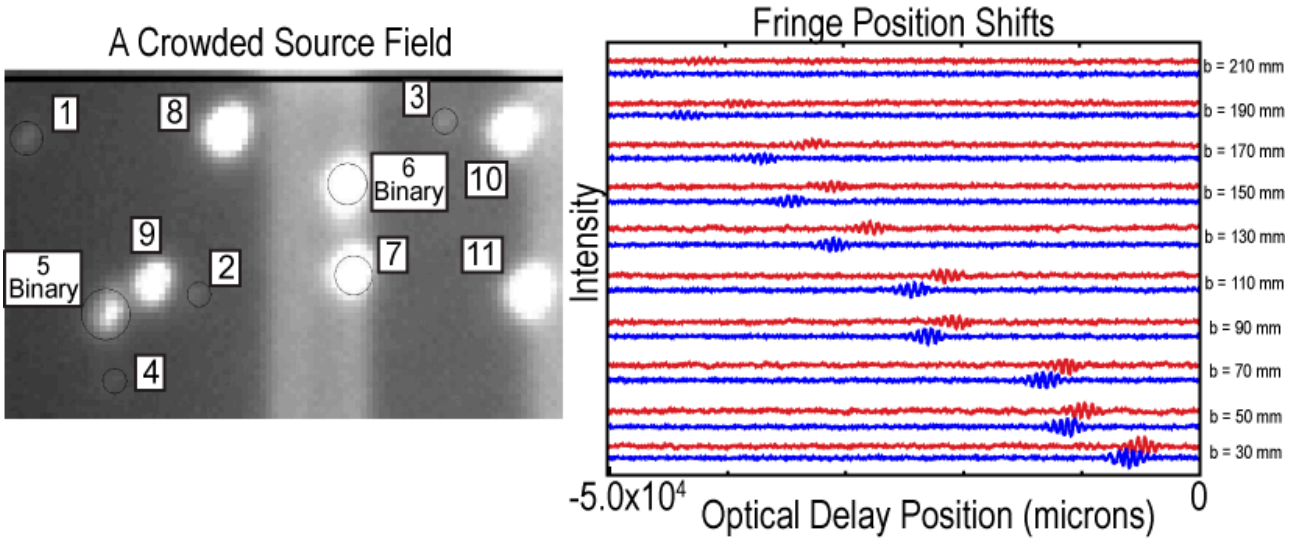

Figure 4: We have acquired data on "Constellation" fields, which include multiple sources with a wide range of pinhole sizes and corresponding brightnesses. An example of one such field is shown in the left panel, above. Within this field, there are 13 individual sources (11 as marked; sources 5 and 6 are binary sources). With WIIT, we obtain fringes for all of the individual sources in the field. As shown in the right panel above, the fringes from individual sources separate and the fringe visibility decreases at longer baselines.

sources increases within the series, to a total separation several times greater than λ/2D (i.e., wide-field separation). These sources were observed with baselines sampling the entire *u-v* plane, and the measurements were shown to be consistent with analytical predictions. Additionally, we explored a variety of other source images, including "constellations", so named because they include a variety of pinholes designed to look like a constellation (such as Hercules, in Figure 4), and targets with 3 or 4 pinhole sources in a single line. In all cases, the measured results have been consistent with expectations (Figure 5). The full *u-v* plane data sets allow us to resolve individual sources, derive their relative locations, determine their individual diameters, and derive the spectrum of the sources for comparison with input "truth images."

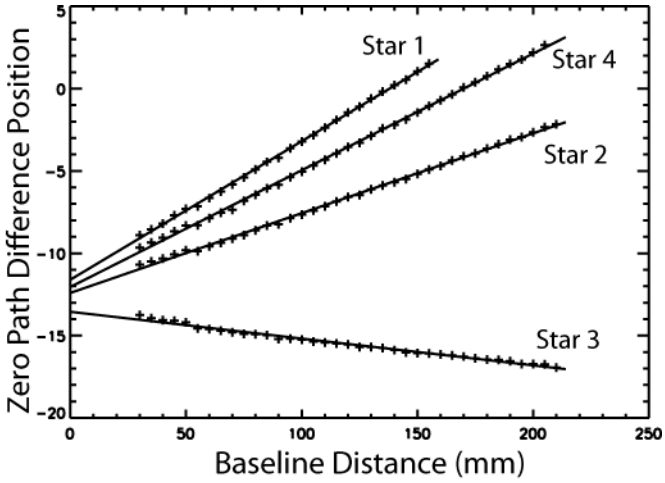

Figure 5: Measurements of the Zero Path Difference (ZPD) point for the fringes produced by different sources allow very precise determination of their relative positions. The slopes of the lines shown here are directly proportional to the angular distances between the sources and the center of the interferometer's field-of-view.

Downloaded From: http://spiedigitallibrary.org/ on 05/24/2017 Terms of Use: http://spiedigitallibrary.org/ss/termsofuse.aspx

In addition to acquiring data for a variety of different spatial distributions, we have acquired data using several different spectral sources. The primary light source used for these data is a white light source. To expand the range of the sources that we can test, we constructed an LED array that allows us to feed the light from up to three different LEDs into the testbed simultaneously. Using the LEDs, we acquired data for a number of the source images using a variety of different input spectra (Figure 6), in order to demonstrate that we can accurately reconstruct even complex spectra from the observed fringes.

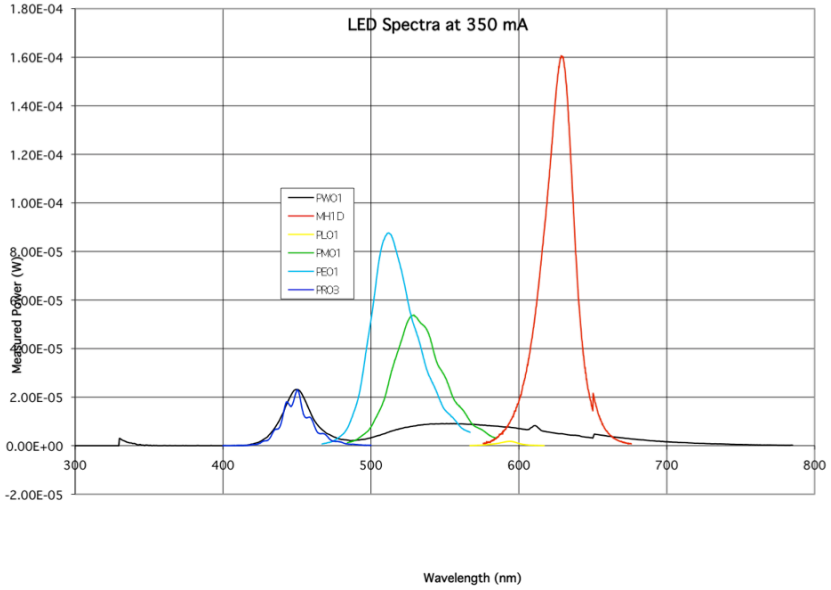

Figure 6: Our LED array provides access to six different illumination profiles. The different LED spectra are shown here.

3. MODELING

We developed a high-fidelity computational model of WIIT using the commercially available FRED optical engineering software. FRED is able to keep track of phase information, allowing for a physically realistic treatment of the coherent rays that traverse multiple paths through an interferometer up to the point of beam combination. Test scenes are represented as a collection of individual monochromatic point sources, randomly distributed spatially over the extended source area. To achieve the desired source spectrum the wavelength of each point source is selected from a probability distribution function shaped like the source spectrum. This Monte Carlo approach has been very effective in modeling the LED and white-light lamp spectra used in actual testbed trials.

Following the experimental approach outlined in Section 1.4, we have modeled both an ideal optical system and a system that incorporates various hardware imperfections known to be present in the testbed.For example, using precise in-lab measurements of WIIT's actual mirror surfaces, we were able to express low- to mid-spatial frequency undulations unique to each mirror as the sum of Zernike polynomials. FRED allows the user to input the appropriate Zernike coefficients for each mirror such that the desired effects are incorporated into the system raytrace. The surface roughness of WIIT's mirrors, with a measured rms amplitude of 1.36 nm, was also integrated into the model. However, in agreement with theory, the resultant scattering of light was found to have a negligible effect on the model results.

An rms wavefront error of the recombined beam of 27.1 nm has been derived from the Zernike coefficients of each mirror. In the future, we will compare analytical predictions for the visibility loss due to this and other significant error terms with loss seen in the model.

Downloaded From: http://spiedigitallibrary.org/ on 05/24/2017 Terms of Use: http://spiedigitallibrary.org/ss/termsofuse.aspx

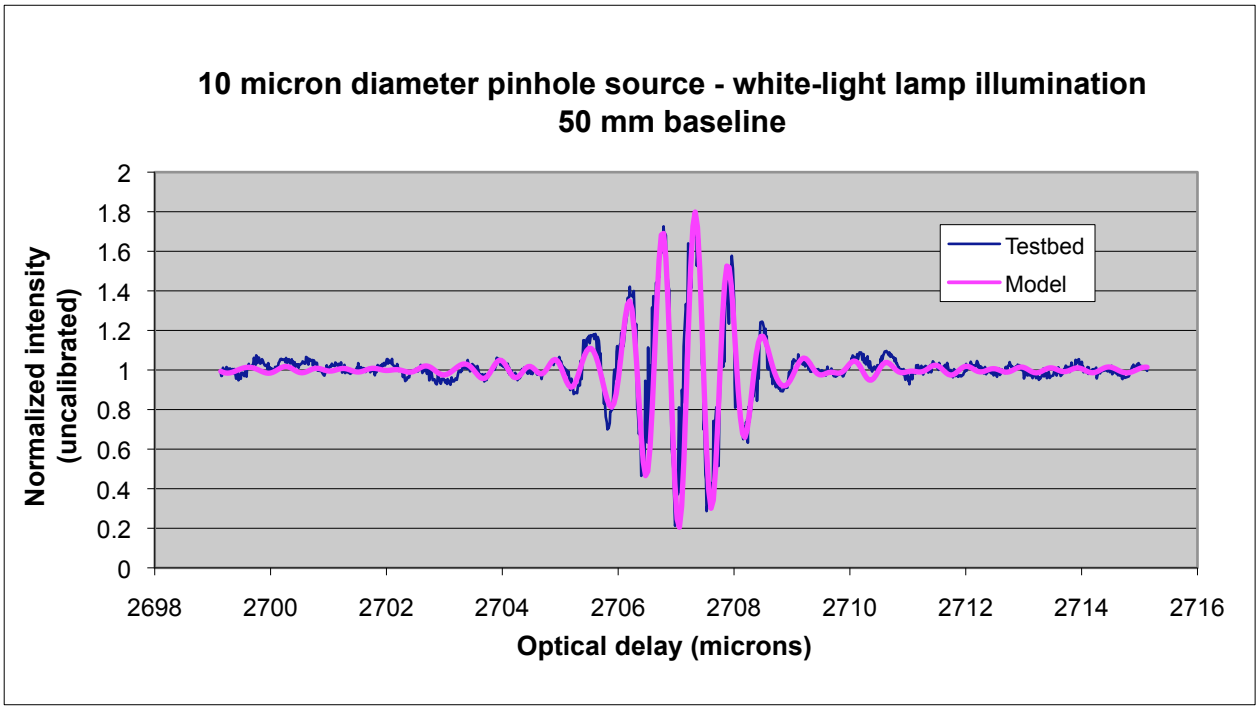

A comparison of the shapes of model and testbed interferograms provides a meaningful measure of the accuracy of the model to date. Figure 6 shows such a comparison, in which the source was a single 10 micron diameter pinhole with a Moritex white-light lamp spectrum observed with a 50 mm baseline. The testbed interferogram has been expanded along

Figure 6: Comparison of a model interferogram (pink) and a testbed interferogram (blue) suggests that the model accurately simulates real testbed performance. The modeled test scene was designed to simulate the same 5-micron pinhole source and white-light lamp spectrum observed by the testbed using the same 50 mm baseline. The testbed interferogram has been expanded along the vertical axis by a factor of 2.9 so as to make the fringe visibility equal to that of the model interferogram. "Normalized intensity" refers to the intensity divided its average value over the entire optical delay range.

the vertical axis by a factor of 2.9, such that the fringe visibility matches that of the model interferogram. Evidently, there is close agreement between model and testbed interferogram shapes. Even some of the features in the wings of the testbed interferogram previously attributed to noise are also present in the model interferogram. Incomplete calibration of the testbed data means we cannot yet compare the visibility of real WIIT interferograms with corresponding model interferograms. Plans for flat-fielding and other calibrations are already in place for the near future. Our aim is to apply appropriate calibration factors and demonstrate that the model and testbed interferograms agree to within the uncertainty associated with statistical noise in the detection process.

After the model has been shown to generate output sufficiently similar to that of the hardware testbed, Monte Carlo methods can be further applied to simulate spatially and spectrally complex astronomical sources that future interferometers like SPIRIT and SPECS would observe. Examples include “deep field” observations of galaxies and planetary debris disks. Modeling of the latter is currently being attempted using three-dimensional probability distributions from a pre-existing debris disk model by M. Kuchner (private communication) which covers seven different wavelength channels.

Eventually, the WIIT model can be scaled to simulate observations in the far-IR and submillimeter wavebands to be covered by BETTII, SPIRIT and SPECS.

Downloaded From: http://spiedigitallibrary.org/ on 05/24/2017 Terms of Use: http://spiedigitallibrary.org/ss/termsofuse.aspx

4. CHIP

Currently in the WIIT testbed, we provide spatial complexity using a 13x13 array of spatial scenes. Input spectra are provided either by a white-light source or by the LEDs (as discussed above). While this scheme has allowed us to demonstrate the fundamentals of the wide-field imaging interferometry technique, the spatially invariant spectrum and spatially invariant intensity within extended objects inherent in this approach have prevented us from considering more complex, astrophysically realistic test scenes. Earlier, we had anticipated overcoming this limitation by using color slides of astronomical scenes. However, this approach had drawbacks, including limited dynamic range and an inability to simulate narrow spectral features.

To provide maximum spatial and spectral flexibility with good dynamic range, we are now pursuing a different approach. We are constructing a Calibrated Hyperspectral Image Projector (CHIP) based on a prototype unit developed by the Optical Technologies Division at NIST (Rice, et al. 2006a; Rice, et al. 2006b). The CHIP uses two digital light processing (DLP®) digital mirror devices (DMD®s) to create a customized, spectrally-diverse scene. One DMD® is used with a prism and a broadband source to create the spectral engine where the columns of the DMD® are mapped to individual wavelengths. Turning individual columns "on" at any given time includes those particular wavelengths in the output spectrum. The number of pixels in each column that are on determines the relative weighting of each wavelength in the output spectrum. The second DMD® creates the spatial scene, in much the same way as a commercial video projector. By synchronizing specific spectral basis functions with the corresponding spatial locations in the scene that contain those spectra, full spatially-spectrally complex images can be constructed and projected into WIIT.

The Goddard-developed CHIP will be capable of producing arbitrary spectra in the band between 380 nm and 780 nm with a spectral resolution of 5 nm. The DMD® technology has a native spatial resolution of 1024 x 768 pixels, with 10.8 micron pixels. Relay optics will match the pupils of the CHIP with WIIT, and de-magnify the scene created by the CHIP to provide a hyperspectral scene to WIIT with features as small as 1 micron (~ 0.2 arc seconds).

5. FUTURE PLANS

We have continued to advance the technique and practice of wide-field imaging interferometry, and we anticipate bringing the technique to TRL 6 by 2012. This requires demonstration of the technique using the WIIT testbed, acquiring astrophysically representative data with the testbed under conditions in which it is functionally equivalent to an interferometer operating in space, a well-understood, high-fidelity computational model that accurately predicts the observed data, and algorithms and code to synthesize wide-field spatial-spectral data cubes from the interferometric data. We have assembled all of the basic ingredients and expect to install the CHIP scene generator in the WIIT by Fall 2010.

Over the next year, we will continue taking data with WIIT in order to continue exploring the fundamental capabilities and practical limitations of the wide-field double-Fourier technique. The new data will be used to test and refine spatial-spectral synthesis algorithms. At the same time, we will continue to model interferometric observations of simple and complex, astrophysically representative scenes in order to probe the fundamental limitations of the technique.

Once we have obtained data for a variety of complex scenes, we will also explore an "on-the-fly" observing mode. "Step-and-stare" is the present mode of data acquisition, where the baseline mirrors are moved to a fixed position and locked in place, and while they are locked, the delay line is scanned to provide fringes on the detector. This is the simplest possible observation mode, but it is not exactly analogous to the operational modes envisaged for future space-based interferometers like SPIRIT. Such interferometers may rotate continuously during operation. By rotating the source stage during data acquisition with WIIT, we can mimic this "on-the-fly" operation. This will lead to some smearing of the fringes as the baseline positions change during a delay line scan, and we will need to adapt our synthesis algorithms and explore how smearing impacts the quality of the reconstructed images.

Downloaded From: http://spiedigitallibrary.org/ on 05/24/2017 Terms of Use: http://spiedigitallibrary.org/ss/termsofuse.aspx

REFERENCES

[1] Rinehart, S., Armstrong, T., Frey, B., Jung, J., Kirk, J., Leisawitz, D., Leviton, D., Lyon, R., Martino, A., Mundy, L., Pauls, T., & Thompson, A. "The Wide-Field Imaging Interferometry Testbed: Result Results," Proc SPIE 6368, 36 (2006).

[2] Rinehart, S.A., "SPECS: The Submillimeter Probe of the Evolution of Cosmic Structure," In *Space Telescopes and Instrumentation I*, Proc. SPIE 6265, 60 (2006).

[3] Harwit, M. et al., "A Kilometer-Baseline Far-Infrared/Submillimeter Interferometer in Space," in *Progress in Astronautics & Aeronautics*, v. 224, ed. M.S. Allen (AIAA: Reston, VA), 301 (2008).

[4] Mariotti, J.-M. & Ridgeway, S.T., "Double Fourier Spatio-Spectral Interferometry – Combining High Spectral and Spatial Resolution in the Near Infrared," A&A, **195**, 350 (1988).

[5] Feinberg, L, Leisawitz, D., Leviton, D., Zhang, X., & Lyon, R, "Design and Plans for a Wide-Filed Imaging Interferometry Testbed," In *Imaging Spectrometry VI*, Proc. SPIE 4132, 365 (2000).

[6] Leisawitz, D., et al. "The Space Infrared Interferometric Telescope (SPIRIT): High-Resolution Imaging and Spectroscopy in the Far-Infrared", J. Adv. Sp. Res. **40**, 689 (2007).

[7] Rinehart, S. A., "The Balloon Experimental Twin Telescope for Infrared Interferometry (BETTII)", in *Optical and Infrared Interferometry II*, Proc. SPIE 7734, 7734-19 (2010).

[8] Rinehart, S., Leisawitz, D., Frey, B., Lyon, R., Maher, S., Memarsadeghi, N., "The Wide-Field Imaging Interferometry Testbed (WIIT)_: Recent Progress and Results," in *Optical and Infrared Interferometry*, Proc. SPIE 7013, 85 (2008).

[9] Leisawitz, D., Frey, B., Leviton, D., Martino, A., Maynard, W., Mundy, L, Rinehart, S., Teng, S., & Zhang, X. "Wide-field Imaging Interferometry Testbed I: Purpose, Pestbed Design, Data, and Synthesis Algorithms", Proc. SPIE, 4852, 255 (2003).

[10] Lyon, R., Leisawitz, D., Rinehart, S., & Memarsadeghi, N., "Wide-Field Imaging Interferometry Image Reconstruction Algorithms," in *Optical and Infrared Interferometry II*, Proc. SPIE 7734, 7734-50 (2010).

[11] Prasad, S. and Kulkarni, S. R. "Noise in optical synthesis images. I. Ideal Michelson interferometer," J. Opt. Soc. Am. A, 6, 1702 (1989).

[12] Rice, J.P., Brown, S.W, Johnson, B.C., & Neira, J.e., "Hyperspectral image projectors for radiometric applications," *Metrologia* **43,** S61-S65 (2006).

[13] Rice, J.P, Brown, S.W. & Neira, J.E., "Development of hyperspectral image projectors," Proc. SPIE **6297,** 629701-629701 (2006).

ACKNOWLEDGEMENTS

Funding for WIIT is provided by NASA Headquarters through the ROSES/APRA program.

Downloaded From: http://spiedigitallibrary.org/ on 05/24/2017 Terms of Use: http://spiedigitallibrary.org/ss/termsofuse.aspx